Double Diffraction at a Pair of Coplanar Skew Edges

Filippo Capolino, *Member, IEEE*, Matteo Albani, Stefano Maci, *Member, IEEE*, and Roberto Tiberio, *Fellow, IEEE*

***Abstract*—A high-frequency solution is presented for the scattering in the near zone by a pair of coplanar skew edges when they are illuminated by a source at a finite distance. The solution is obtained by using a spherical-wave spectral representation of the first-order diffracted field from each edge. The final closed-form asymptotic solution includes terms up to the second order. It is shown that this second-order contribution is of the same order as the first one in overlapping transition regions. Moreover, the solution is cast in a convenient form, which is also directly applicable to treat the case when the two edges share a common face for both soft and hard boundary conditions. By choosing appropriate reference systems, the formulation for the scalar case is directly used to construct the solution of the more general electromagnetic problem for an arbitrarily polarized incident field. Numerical results are presented and discussed.**

***Index Terms*— Electromagnetic scattering, geometrical theory of diffraction.**

I. Introduction

THE high-frequency description of diffraction mechanisms at a pair of interacting edges has been thoroughly considered in the literature. In several practical applications, the ray-field representation of the scattering phenomenon involves significant contributions from doubly diffracted ray fields from the two edges (i.e., when the leading singly diffracted ray fields are shadowed). It is rather well known that the subsequent application of the ordinary uniform theory of diffraction (UTD) coefficients [1] fails when the second edge is located in the transition region of the first edge and the diffracted field is calculated at the shadow boundary (SB) or reflection boundary (RB) of the second edge. This is due to the rapid spatial variation and the nonray optical behavior of the incident field at the second edge after diffracting from the first. The angular range of those incidence and observation aspects where the above condition may occur broadens as the distance between the two edges and their distances from the source and the observation points decrease. The problem of diffraction by two parallel edges was first investigated in [2]–[4]. In [5], diffraction coefficients were obtained, by using a spectral extension of the UTD, for plane wave incidence and far-field observation. A more general solution for the same problem was developed in [6]; there, again, a spectral formulation was used. A different formulation based on the physical theory of diffraction (PTD) was presented in [7] and [8]. A significant improvement was given in [9] and [10], where the problem of skewed coplanar wedges was analyzed.

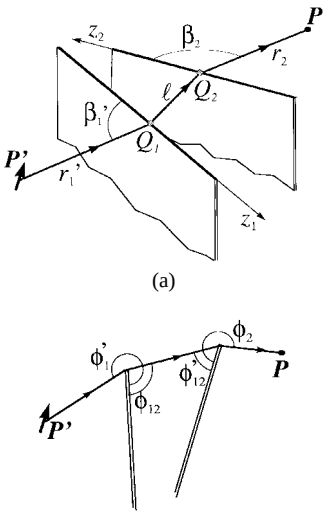

Fig. 1. Geometry at two skew half planes. (a) Angles with respect to the edges. (b) Transverse angles.

In this paper, a closed-form high-frequency solution is presented for describing double diffraction (DD) mechanisms in the near zone of a pair of skew knife-edges, when they are illuminated by a spherical wave. For the sake of simplicity, in Section II, the scalar case is formulated, when either hard or soft boundary conditions (BC) are imposed on the faces of the two half-planes. The DD analysis, consists of two steps. First, the spherical wave spectrum of the diffracted field from the first wedge [11] when it is illuminated by a spherical source is used as the incident field at the second wedge. Next, the near-field response of the second edge to any spherical spectral source is used to obtain a double integral representation for the doubly diffracted field [5]. In Section III, this integral is asymptotically evaluated to determine the desired closed-form (ray-optical) expression. This asymptotic evaluation leads to transition functions involving generalized Fresnel integrals. In Section IV, the scalar result is used for constructing the solution of the more general electromagnetic case.

The behavior of the present solution is thoroughly examined in Section V. Furthermore, there, the practically interesting case of two edges sharing common faces is explicitly considered also to provide a neat physical insight.

II. Formulation

Let us consider a pair of coplanar skew edges, illuminated by a spherical incident field. Our description of the DD mechanism is constructed as the superposition of two analogous mechanisms; a diffracted field from edge 2 when

Manuscript received October 20, 1995; revised January 27, 1997. This work was supported by the European Space Agency (ESA-ESTEC), The Netherlands.

F. Capolino, M. Albani, and R. Tiberio are with the College of Engineering, University of Siena, Siena, 53100 Italy.

S. Maci is with the Department of Electronics Engineering, University of Florence, Florence, 50139 Italy.

Publisher Item Identifier S 0018-926X(97)05591-9.

it is illuminated by the diffracted field from edge 1 (12), and that from edge 1 when it is illuminated by edge 2 (21). In the following, contribution 12 is explicitly considered; it is then a straightforward matter to obtain the corresponding expression for contribution 21. It is useful to define an edge-fixed spherical coordinate system (r_i, β_i, ϕ_i) [1] at each edge $(i = 1, 2)$ with their origins at the two diffraction points Q_i that are dictated by the generalized Fermat principle for this double diffraction mechanism, as depicted in Fig. 1. Also, let us denote by $P'(\phi_1') \equiv (r_1', \pi - \beta_1', \phi_1')$ the source point and by ℓ the distance between Q_1 and Q_2. A $e^{j\omega t}$ time dependence is assumed and suppressed.

For the sake of simplicity, the scalar case is treated first; either hard or soft BC may be imposed on the planar faces at the edges. It will be shown that the high-frequency solutions for the two scalar cases are directly used to construct the solution for the electromagnetic case. The field at any point $P(\phi_1) \equiv (r_1, \beta_1, \phi_1)$ from the point source at $P'(\phi_1')$ is expressed as

$$\psi\{P(\phi_1), P'(\phi_1')\} = \frac{e^{-jk|P(\phi_1) - P'(\phi_1')|}}{4\pi|P(\phi_1) - P'(\phi_1')|}. \tag{1}$$

The diffracted field at any point $P(\phi_1)$ from the edge 1 (when it is illuminated by the spherical wave) may be conveniently represented as [11], [12]

$$\psi_1^d = \frac{1}{2\pi j} \int_{C_{\alpha_1}} \psi\{P(\phi_1), P'(\alpha_1 \pm \pi)\} G_1(\phi_1', \alpha_1)\, d\alpha_1 \tag{2}$$

where the $\pm$ sign applies to $\phi_1 \lessgtr \pi$ and the contour of integration C_{α_1} is defined along $(-j\infty, \pi + j\infty)$. The geometrical optics (GO) poles are excluded from this treatment. They indeed provide singly diffracted field contributions that are accounted for by a standard UTD formulation. In the case of the half plane

$$G_1(\phi', \phi) = -\frac{1}{2} \sum_{m=1}^{2} (\mp 1)^m \sec\left(\frac{\phi' - (-1)^m \phi}{2}\right) \tag{3}$$

where $-$ $(+)$ refers to the soft (hard) BC.

The integrand in (2) is interpreted as the field of spectral spherical sources localized at $P'(\alpha_1 \pm \pi) \equiv (r_1', \pi - \beta_1', \alpha_1 \pm \pi)$. Next, these spectral spherical sources are used to illuminate the second edge. To this end, ϕ_1 is evaluated at ϕ_{12}, which is the azimuthal coordinate of Q_2 measured in the system at edge 1 (Fig. 1). A pictorial representation of this mechanism is shown in Fig. 2, in which only the spectral sources with real values of α_1 are depicted. Thus, each spherical source provides a diffracted field contribution from edge 2 at any point $P(\phi_2) \equiv (r_2, \beta_2, \phi_2)$. Such a contribution is obtained by analytically continuing into complex space the formulation (2). For the sake of convenience, this same contribution is calculated by invoking reciprocity, i.e., the diffracted field from edge 2 at $P'(\alpha_1 \pm \pi)$ due to a point source at $P(\phi_2)$. This procedure leads to

$$\psi_2^d(\alpha_1) = \frac{1}{2\pi j} \int_{C_{\alpha_2}} \psi\{P'(\alpha_1 \pm \pi), P(\alpha_2 \pm \pi)\} \times G_2(\phi_2, \alpha_2)\, d\alpha_2 \tag{4}$$

in which $P(\alpha_2 \pm \pi) \equiv (r_2, \pi - \beta_2, \alpha_2 \pm \pi)$, and the contour C_{α_2} has the same definition as C_{α_1}. The spectral response of edge 2 is then described by the integrand of (2) after replacing therein $\psi\{P'(\alpha_1 \pm \pi), P(\phi_1)\}$ by $\psi_2^d(\alpha_1)$. By spectral synthesis, the desired double spectral integral representation for the doubly diffracted field ψ_{12}^{dd} is obtained. To this end, the convenient notation is introduced in (5), shown at the bottom of the page, in which

$$\begin{aligned} g_1(\eta_1) &= \sin^2\beta_1'(\cos\eta_1 - 1) \\ g_2(\eta_2) &= \sin^2\beta_2(\cos\eta_2 - 1) \\ f(\eta_1, \eta_2) &= g_1(\eta_1) + g_2(\eta_2) - \epsilon_{12}\sin\beta_1'\sin\beta_2 \\ &\quad \times [\cos(\beta_1' + \epsilon_{12}\beta_2)(\cos\eta_1 - 1)(\cos\eta_2 - 1) \\ &\quad + \sin\eta_1 \sin\eta_2] \\ \epsilon_{12} &= -\mathrm{sgn}(\hat{z}_1 \cdot \hat{z}_2). \end{aligned} \tag{6}$$

This indeed is used to provide an explicit expression for ψ within the integral representation of $\psi_2^d(\alpha_1)$ in (4) so that

$$\psi_{12}^{dd} = -\frac{1}{4\pi^2} \int_{C_{\alpha_1}} \int_{C_{\alpha_2}} \frac{e^{-jkR(\alpha_1 - \phi_{12}, \alpha_2 - \phi_{12}')}}{4\pi R(\alpha_1 - \phi_{12}, \alpha_2 - \phi_{12}')} \times G_1(\phi_1', \alpha_1) G_2(\phi_2, \alpha_2)\, d\alpha_1\, d\alpha_2 \tag{7}$$

where ϕ_{12} has been defined earlier and ϕ_{12}' is the azimuthal coordinate of Q_1 measured in the system at edge 2 (Fig. 1). It is rather apparent that (7) explicitly satisfies reciprocity. Also, it is worth pointing out that the pole singularities of the spectra $G_1(\phi_1', \alpha_1)$ and $G_2(\alpha_2, \phi_2)$ independently occur in the two variables of integration. Finally, it is useful to introduce the change of variables from $(\alpha_1 - \phi_{12})$ to α_1 and from $(\alpha_2 - \phi_{12}')$ to α_2 so that

$$\psi_{12}^{dd} = -\frac{1}{4\pi^2} \int_{-j\infty}^{j\infty} \int_{-j\infty}^{j\infty} \frac{e^{-jkR(\alpha_1, \alpha_2)}}{4\pi R(\alpha_1, \alpha_2)} \times G_1(\phi_1', \alpha_1 + \phi_{12}) G_2(\phi_2, \alpha_2 + \phi_{12}')\, d\alpha_1\, d\alpha_2 \tag{8}$$

in which the original contours of integration have been deformed onto their imaginary axis, without capturing any of the poles that occur on the real axis. This latter expression is found suitable for asymptotic evaluation, which is presented in the next section.

III. High-Frequency Solution

The double spectral-integral representation for ψ_{12}^{dd} is now asymptotically evaluated to find a high-frequency expression for this DD mechanism. To this end, it is seen that the integral in (8) exhibits a two-dimensional, stationary phase point at $(\alpha_1, \alpha_2) = (0, 0)$. Its asymptotically dominant contribution provides the doubly diffracted ray-field contribution, which is the purpose of this paper. It should be noted, however, that a

$$R(\eta_1, \eta_2) = \sqrt{(r_1' + \ell + r_2)^2 + 2r_1'\ell g_1(\eta_1) + 2r_2\ell g_2(\eta_2) + 2r_1'r_2 f(\eta_1, \eta_2)} \tag{5}$$

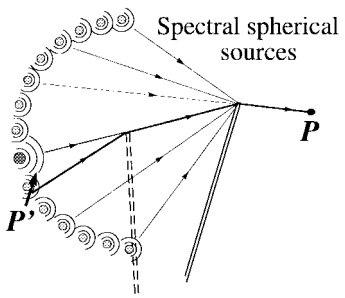

Fig. 2. Pictorial representation of the field diffracted from the first edge in terms of spectral spherical sources radiating in free space; the marked source denotes the stationary direction in the diffraction integral.

further stationary point may occur that is associated with a field contribution emanating from the intersection between the two coplanar edges if it exists in the actual structure. The treatment of this vertex contribution is beyond the scope of this paper and will not be considered here; thus, we will assume that both the DD points are far from any vertex point. A high-frequency description of diffraction mechanisms at a vertex may be found in [13]–[15]. As mentioned earlier, the integrand in (8) exhibits pole singularities that independently occur in the two spectral variables. These poles may occur close to and at the stationary point. Thus, they have to be appropriately accounted for. It is now convenient to express the spectral functions G_i as the sum of their even and odd parts [5], i.e.,

$$G_i = \mp\frac{1}{2}\sum_{m=1}^{2}\frac{(\pm 1)^m \sin\frac{\Phi_i^m}{2}\cos\frac{\alpha_i}{2} + (\mp 1)^m \cos\frac{\Phi_i^m}{2}\sin\frac{\alpha_i}{2}}{\cos^2\frac{\alpha_i}{2} - \cos^2\frac{\Phi_i^m}{2}} \tag{9}$$

where $G_1 = G_1(\phi_1', \alpha_1 + \phi_{12}), G_2 = G_2(\alpha_2 + \phi_{12}', \phi_2), \Phi_i^m$ is either

$$\Phi_1^p = \phi_1' + (-1)^p\phi_{12} + \pi \quad (i = 1,\ m = p) \tag{10}$$

or

$$\Phi_2^q = \phi_2 + (-1)^q\phi_{12}' + \pi \quad (i = 2,\ m = q) \tag{11}$$

and the upper (lower) sign applies to the hard (soft) case.

It will be seen that these even and odd parts provide two different asymptotic contributions that have their own specific physical meaning and render the final solution directly applicable to any double knife-edge configuration, including the case when the two edges share common faces.

The details of the asymptotic approximation of expression (8) are presented in the Appendix, where it is shown that the desired high-frequency solution for the double diffraction mechanism 12 is

$$\psi_{12}^{dd} \sim \psi\{P', Q_1\}A(r_1', \ell, r_2)D_{12}^{s,h} \tag{12}$$

in which

$$\begin{aligned}\psi\{P', Q_1\} &= \frac{e^{-jkr_1'}}{4\pi r_1'}\\ A(r_1', \ell, r_2) &= \frac{\sqrt{r_1'}}{\sqrt{\ell r_2}\sqrt{r_1' + \ell + r_2}}e^{-jk(\ell + r_2)}\end{aligned} \tag{13}$$

denote the incident field at edge 1 and the spreading factor, respectively. Furthermore, in (12), $D_{12}^{s,h}$ are the diffraction coefficients for the hard (h) and soft (s) cases that are expressed as

$$D_{12}^{s,h} = \tilde{D}_{12}^{s,h} + \tilde{\tilde{D}}_{12}^{s,h} \tag{14}$$

in which

$$\tilde{D}_{12}^{s,h} = \frac{1}{8\pi jk\sin\beta_1'\sin\beta_2} \cdot \sum_{p,q=1}^{2}(\mp 1)^{p+q}\frac{1}{\sin\left(\frac{\Phi_1^p}{2}\right)\sin\left(\frac{\Phi_2^q}{2}\right)} \cdot \tilde{T}(a_p, b_q, w) \tag{15}$$

and

$$\tilde{\tilde{D}}_{12}^{s,h} = -\frac{\epsilon_{12}}{32\pi k^2\ell\sin^2\beta_1'\sin^2\beta_2} \cdot \sum_{p,q=1}^{2}(\pm 1)^{p+q}\frac{\cos\left(\frac{\Phi_1^p}{2}\right)\cos\left(\frac{\Phi_2^q}{2}\right)}{\sin^2\left(\frac{\Phi_1^p}{2}\right)\sin^2\left(\frac{\Phi_2^q}{2}\right)} \cdot \tilde{\tilde{T}}(a_p, b_q, w) \tag{16}$$

where ϵ_{12} is the same defined in (6) and the upper (lower) sign applies to the soft (hard) case. Equations (15) and (16) involve the transition functions

$$\begin{aligned}\tilde{T}(a,b,w) &= \frac{2\pi jab}{\sqrt{1-w^2}}\left[\mathcal{G}\left(a, \frac{b+wa}{\sqrt{1-w^2}}\right) + \mathcal{G}\left(b, \frac{a+wb}{\sqrt{1-w^2}}\right)\right.\\ &\quad \left. + \mathcal{G}\left(a, \frac{b-wa}{\sqrt{1-w^2}}\right) + \mathcal{G}\left(b, \frac{a-wb}{\sqrt{1-w^2}}\right)\right]\end{aligned} \tag{17}$$

and

$$\begin{aligned}\tilde{\tilde{T}}(a,b,w) &= \frac{-4\pi(ab)^2}{w\sqrt{1-w^2}}\left[\mathcal{G}\left(a, \frac{b+wa}{\sqrt{1-w^2}}\right) + \mathcal{G}\left(b, \frac{a+wb}{\sqrt{1-w^2}}\right)\right.\\ &\quad \left. - \mathcal{G}\left(a, \frac{b-wa}{\sqrt{1-w^2}}\right) - \mathcal{G}\left(b, \frac{a-wb}{\sqrt{1-w^2}}\right)\right]\end{aligned} \tag{18}$$

respectively, that are the same as those introduced in [16] for the problem of double diffraction at a thick screen; in (17) and (18), $\mathcal{G}$ is the Generalized Fresnel Integral (GFI)

$$\mathcal{G}(x,y) = \frac{y}{2\pi}e^{jx^2}\int_x^\infty \frac{e^{-j\tau^2}}{\tau^2 + y^2}\,d\tau \tag{19}$$

which is defined for negative arguments as $\mathcal{G}(x,-y) = \mathcal{G}(-x,y) = -\mathcal{G}(x,y)$. A very simple algorithm for computing the GFI in (19) is suggested in [14]. The arguments of the transition functions in (15) and (16) are defined as

$$\begin{aligned}a_p &= \sqrt{2k}\sin\beta_1'\sqrt{\frac{r_1'\ell}{r_1' + \ell}}\sin\left(\frac{\Phi_1^p}{2}\right),\\ b_q &= \sqrt{2k}\sin\beta_2\sqrt{\frac{r_2\ell}{r_2 + \ell}}\sin\left(\frac{\Phi_2^q}{2}\right)\end{aligned} \tag{20}$$

and

$$w = \sqrt{\frac{r_1'r_2}{(r_1' + \ell)(\ell + r_2)}} \tag{21}$$

in which Φ_1^p and Φ_2^q are defined in (10) and (11).

It is rather apparent that the same overall process leading to the high-frequency expression (12), is applicable to find the corresponding expression for mechanism 21. After having determined the relevant ray-path, it is a straightforward matter to obtain the explicit expression for ψ_{21}^{dd}.

Before discussing the behavior of the high-frequency solution presented so far, it is useful to explicitly consider the extension of the present scalar solution to the electromagnetic case.

IV. Electromagnetic Diffraction Coefficient

As was done in [5], [6], and [9], the solution of the scalar problem can be directly used to construct a solution for the corresponding electromagnetic problem of an arbitrarily polarized spherical wave; its representation in the standard format of the UTD is given next.

A simple, compact dyadic expression for the doubly diffracted field is obtained by conveniently choosing the reference systems. To this end, let us consider the two edge fixed coordinate systems [1] at the two diffraction points Q_1 and Q_2, with unit vectors $(\hat{r}_1', \hat{\beta}_1', \hat{\phi}_1')$ from the source to Q_1, and $(\hat{r}_2, \hat{\beta}_2, \hat{\phi}_2)$ from Q_2 to the observation point. Accordingly, let us denote by $\boldsymbol{E}^i(Q_1) \equiv (E^i_{\beta_1'}, E^i_{\phi_1'})$ the arbitrarily polarized, incident electric field at Q_1 and by $\boldsymbol{E}^{dd}(r_1', r_2) \equiv (E^{dd}_{\beta_2}, E^{dd}_{\phi_2})$ the doubly diffracted electric field from mechanism 12. It is then found that

$$\boldsymbol{E}^{dd}(r_1', r_2) = \boldsymbol{E}^i(Q_1)\boldsymbol{\mathcal{D}}_{12}A(r_1', \ell, r_2) \tag{22}$$

in which the dyadic double diffracted coefficient is represented as

$$\boldsymbol{\mathcal{D}}_{12} = \epsilon_{12}\left(\hat{\beta}_1'\hat{\beta}_2 D_{12}^s + \hat{\phi}_1'\hat{\phi}_2 D_{12}^h\right) \tag{23}$$

where $D_{12}^{s,h}$ are the same as those obtained so far for the corresponding scalar problems.

V. Analysis

It is now interesting to investigate the properties of the DD contribution described by (12) at various incidence and observation aspects. In particular, the following issues will be addressed: 1) the asymptotic order of magnitude of the terms provided by the DD contribution is analyzed and its limit at the shadow boundaries are explicitly calculated to show that our solution exhibits the appropriate discontinuities to compensate for the GO shadowing of the singly diffracted fields; furthermore it is seen that this formulation nicely recovers the known solution in the plane wave, far-field limit [5] and 2) the case of the plane angular sector is presented as a limit of the general solution.

A. Asymptotic Behavior and Shadow Boundary Limits

The DD ray field ψ_{12}^{dd} consists of the sum of two terms associated with $\tilde{D}_{12}^{s,h}$ and $\tilde{\tilde{D}}_{12}^{s,h}$. For the sake of convenience, let us denote them by $\tilde{\psi}_{12}^{dd}$ and $\tilde{\tilde{\psi}}_{12}^{dd}$, respectively. As can be easily inferred from the asymptotic analysis discussed in the Appendix, the same expressions, but with both $\tilde{T}$ and $\tilde{\tilde{T}}$ equal unity, would have been obtained by a simple nonuniform stationary phase approximation of the spectral integral representation of ψ_{12}^{dd}. Such a nonuniform solution would provide an appropriate description of this DD mechanism when neither the second edge nor the observation point falls into its relevant transition region, i.e., that associated with either the first or the second edge, respectively. In this case, $\tilde{\psi}_{12}^{dd}$ is of order k^{-1} and $\tilde{\tilde{\psi}}_{12}^{dd}$ of order k^{-2}, with respect to the direct incident field. This suggests that the contribution $\tilde{\tilde{\psi}}_{12}^{dd}$ essentially describes a slope diffraction effect. Indeed, the same nonuniform expressions would result from a straightforward application of GTD double diffraction ($\tilde{\psi}_{12}^{dd}$) and slope diffraction ($\tilde{\tilde{\psi}}_{12}^{dd}$). When either the second edge or the observation point approaches the relevant shadow boundary (SB), $\tilde{\psi}_{12}^{dd}$ provides a contribution of the same order $k^{-1/2}$ as a singly diffracted field and $\tilde{\tilde{\psi}}_{12}^{dd}$ is of order k^{-1}. When the two transition regions overlap, i.e., when both the source and the observation point approach grazing, both $\tilde{\psi}_{12}^{dd}$ and $\tilde{\tilde{\psi}}_{12}^{dd}$ are of the same order k^0 as the direct illuminating field. Such an effective description of the expected ray field behavior is neatly provided by the transition functions $\tilde{T}$ and $\tilde{\tilde{T}}$, as shown hereafter.

Let us consider first the case when the observation point crosses the plane containing edges 1 and 2. There, the singly diffracted field from edge 1 is discontinuous, due to the shadowing by edge 2. At this same aspect, $\phi_2 = \phi_{12}' + \pi$ so that $\Phi_2^1 = 2\pi$ and consequently $b_1 = 0$. When approaching this aspect, both $q = 1$ terms in (15) are in their transition regions, so that (as shown in the Appendix)

$$\tilde{\psi}_{12}^{dd} = \frac{1}{2}\mathrm{sgn}(b_1)\frac{\psi\{P', Q_1\}}{2\sqrt{2\pi jk}\sin\beta_1'}\frac{\sqrt{r_1'}e^{-jk(\ell+r_2)}}{\sqrt{(\ell+r_2)(r_1'+\ell+r_2)}} \cdot \sum_{p=1}^{2} F\left(\frac{a_p^2}{1-w^2}\right)\frac{(\mp 1)^{p+1}}{\sin\left(\frac{\Phi_1^p}{2}\right)} + O(k^{-1}) \tag{24}$$

where F is the UTD transition function [1]. The leading term of (24) is easily recognized as $\frac{1}{2}\mathrm{sgn}(b_1)$ times the standard UTD expression for the singly diffracted field from edge 1, so that its discontinuity is precisely compensated. Higher order terms in (24) as well as $\tilde{\tilde{\psi}}_{12}^{dd}$, are continuous and well behaved.

Let us consider next the case when the source approaches grazing illumination aspects of the two edges. There, $a_1 \to 0$; indeed, when the source lies on the plane of the two edges, $\phi_1' = \pi + \phi_{12}$ so that $\Phi_1^1 = 2\pi$. The behavior of $\tilde{\psi}_{12}^{dd}$ is similar to that described by (24), where now the role of the parameters relevant to the observation is interchanged with that of the illumination. This allows $\tilde{\psi}_{12}^{dd}$ to provide the

appropriate compensation of the discontinuity of the singly diffracted field from edge 2, due to the shadowing by edge 1.

When the observation point also lies on this same plane ($\phi_2 = \phi_{12}' + \pi$), the $pq = 11$ term provides the leading contribution

$$\tilde{\psi}_{12}^{dd} = \frac{1}{4}\mathrm{sgn}(a_1 b_1)\frac{e^{-jk(r_1'+\ell+r_2)}}{4\pi(r_1'+\ell+r_2)} + O(k^{-1/2}). \tag{25}$$

Equations (24) and (25) guarantee the continuity of the total field under any conditions, across $\phi_1' = \phi_{12} + \pi$ and $\phi_2 = \phi_{12}' + \pi$.

In the Appendix, it is shown that ψ_{12}^{dd} provides a significant slope diffraction contribution; in particular, when both $\phi_1' - \phi_{12} = \pi$ and $\phi_2 - \phi_{12}' = \pi$

$$\tilde{\psi}_{12}^{dd} = \frac{1}{2\pi}\mathrm{tg}^{-1}\left(\sqrt{\frac{r_1' r_2}{\ell(r_1'+\ell+r_2)}}\right) \cdot \frac{e^{-jk(r_1'+\ell+r_2)}}{4\pi(r_1'+\ell+r_2)} + O(k^{-1}) \tag{26}$$

which is of the same order as $\tilde{\psi}_{12}^{dd}$ in (25). Equations (25) and (26) demonstrate that the present solution recovers the leading term of the rigorous asymptotic series expansion of the exact solution for two staggered parallel half-planes [4], [17].

The appropriate behavior of our formulation is summarized in the example presented in Fig. 3. There, calculations of the total field are plotted for a scalar point source placed at finite distance from the from two skewed half-planes with hard BC. The relevant geometry and the scan plane are depicted in the inset. The source is placed on the plane containing the two edges, so that the trailing edge is certainly illuminated by a transition region field from the leading edge. Calculations have been performed for various Ω angles between the two edges to show that smooth, continuous, and well behaved curves are obtained even for small distances ℓ between diffraction points. Also, it is found that our calculations (in the limit for $\Omega \to 0$) smoothly blend into the corresponding UTD solution for a single half-plane. This somewhat emphasizes the robustness of the present high-frequency solution and suggests that in general this solution fails gracefully as the distance between the double diffraction points vanishes. We just note that analogously well-behaved results have been obtained for soft BC of the half-planes.

So far, it is worth pointing out that when the source and the observation points move to infinity the present closed-form solution for the doubly diffracted field recovers the plane wave far-field solution obtained in [5]. Indeed, when both r_1' and $r_2 \to \infty$, $w \to 1$; as a consequence, the transition functions $\tilde{T}$ and $\tilde{\tilde{T}}$ may be expressed in terms of Fresnel integrals to give

$$\tilde{T}(a_p, b_q, 1) = \frac{b_q^2 F(a_p^2) - a_p^2 F(b_q^2)}{b_q^2 - a_p^2} \tag{27}$$

$$\tilde{\tilde{T}}(a_p, b_q, 1) = 2j a_p^2 b_q^2 \frac{F(b_q^2) - F(a_p^2)}{b_q^2 - a_p^2} \tag{28}$$

where F is the standard UTD transition function [1] and $a_p = \sqrt{2k\ell}\sin\beta_1'\sin(\frac{\Phi_1^p}{2})$, $b_q = \sqrt{2k\ell}\sin\beta_2\sin(\frac{\Phi_2^q}{2})$. Using (27) and (28) yields the same formulation as that defined in [5] for parallel edges.

B. Plane-Angular Sector

A configuration that is interesting for its practical relevance is the plane angular sector; this can be seen as a particular case of the general solution when the two edges share common faces. This configuration deserves specific attention because the doubly diffracted contribution arises from a field that, after diffracting from the first edge, propagates along the surface

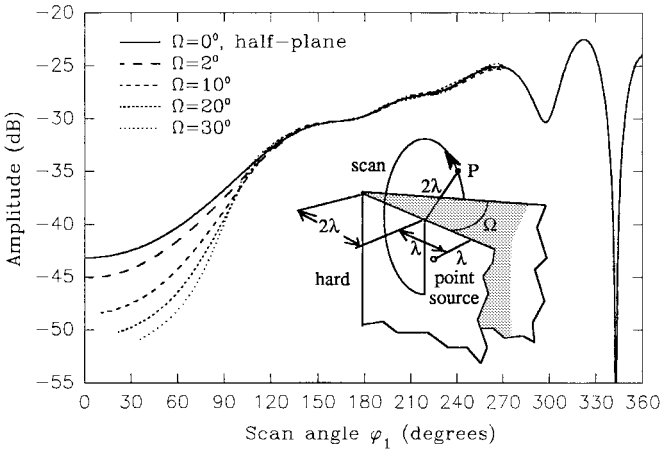

Fig. 3. Total field of a source point placed at a finite distance from the edges of two skewed half-planes with hard BC for various angles (Ω).

joining the two edges. Thus, dealing with either soft or hard BC has a significant impact on the behavior of the field as well as on its ray-field representation.

Owing to the occurrence of $\Phi_1^1 = \Phi_1^2 = \phi_1' + \pi$ and $\Phi_2^1 = \Phi_2^2 = \phi_2 + \pi$, one has $a_1 = a_2 = a$ and $b_1 = b_2 = b$ in (20) and the summation of the four terms in (15) and (16) reduces to a single compact term. To obtain the appropriate formulation, it should be noted that the total doubly diffracted ray field from edge 2 arises from two simultaneous incident fields that propagate along the upper and lower faces, after diffracting at edge 1. Each one of these two fields which effectively impinges on the second edge, is described by one half of the field diffracted by the first edge [5], [9]. Also, it is seen that both contributions arising from the above propagation mechanisms have the same resulting expressions. Finally, after noting that $\tilde{D}_{12}^s = 0$ and $\tilde{\tilde{D}}_{12}^h = 0$, it is found that the diffraction coefficients for describing the total doubly diffracted field relevant to the interaction mechanism 12, nicely reduce to

$$D_{12}^h = \tilde{D}_{12}^h = \frac{1}{2\pi jk\sin\beta_1'\sin\beta_2} \cdot \frac{1}{\cos\left(\frac{\phi_1'}{2}\right)\cos\left(\frac{\phi_2}{2}\right)} \cdot \tilde{T}(a,b,w) \tag{29}$$

and

$$D_{12}^s = \tilde{\tilde{D}}_{12}^s = -\frac{\epsilon_{12}}{8\pi k^2 \sin^2\beta_1'\sin^2\beta_2} \cdot \frac{\sin\left(\frac{\phi_1'}{2}\right)\sin\left(\frac{\phi_2}{2}\right)}{\cos^2\left(\frac{\phi_1'}{2}\right)\cos^2\left(\frac{\phi_2}{2}\right)} \cdot \tilde{\tilde{T}}(a,b,w) \tag{30}$$

where

$$a = \sqrt{2k}\sin\beta_1'\sqrt{\frac{r_1'\ell}{r_1'+\ell}}\cos\left(\frac{\phi_1'}{2}\right)$$

$$b = \sqrt{2k}\sin\beta_2\sqrt{\frac{r_2\ell}{r_2+\ell}}\cos\left(\frac{\phi_2}{2}\right). \tag{31}$$

The above results provide a neat physical insight into the ray-field picture adopted in this paper. Indeed, there is a

correspondence between both the contributions $\tilde{\psi}_{12}^{dd}$ and $\tilde{\tilde{\psi}}_{12}^{dd}$ of the general solution and the DD contribution of the plane angular sector for hard and soft BC, respectively.

It is rather apparent that in the hard case, the field propagating along the surface after diffracting from the first edge experiences a discontinuity at grazing aspects of observation, which is expected to be compensated by the DD contribution. Indeed, $\tilde{D}_{12}^{h}$ exhibits a discontinuity, which is just the opposite of that of the singly diffracted field. This not only provides a precise discontinuity compensation but also causes the scattered field to vanish, as expected from physical inspection. A similar behavior occurs at grazing illumination aspects, $\phi_1' = \pi$.

In the soft case the field propagating along the surface vanishes but exhibits a rapid spatial variation; thus, a strong dominant slope diffraction effect occurs. Also, at grazing observation aspects, the singly diffracted field vanishes so that only a continuous slope contribution is appropriate.

To illustrate the effectiveness of (29) and (30), Fig. 4 shows the total field of an elementary electric dipole placed at a finite distance from a perfectly conducting strip of 0.5λ width. As shown in the inset of the same figure, the dipole is placed at 5° from the plane containing the strip and at 1.75λ from the strip axis, so that the second edge is illuminated by the transition region field from the first edge. Fig. 4(a) and (b) is relevant to the cases in which the dipole is either orthogonal (hard case) or parallel (soft case) to the edges. Results from this formulation (continuous line) are compared with those from first-order UTD (dash-dotted line) and from the method of moments (MoM, dashed line). In the hard case, the first-order UTD field exhibits an expected noticeable jump discontinuity at grazing aspect. This discontinuity is precisely compensated by the second-order diffraction mechanism introduced here; the results are in very good agreement with those from MoM, except maybe at 60° and 305°, where our solution provides deeper minima; higher order diffraction mechanisms may provide the appropriate improvements. In the soft case, the first-order UTD predicts a null at grazing as expected and introducing doubly diffracted contribution provides excellent agreement with the MoM prediction.

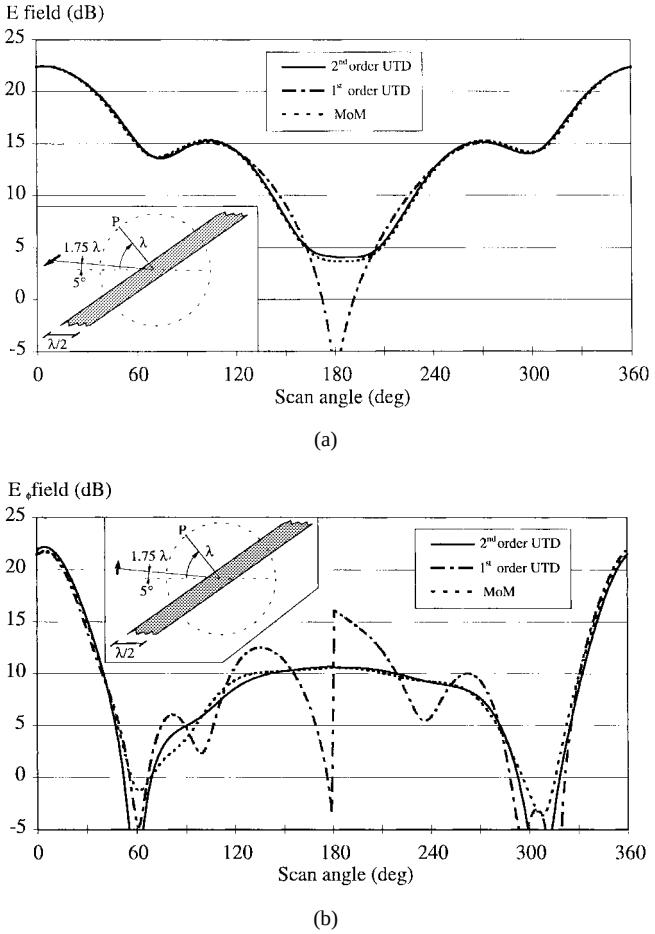

Fig. 4. Electric field of an elementary electric dipole placed at a finite distance from a perfectly conducting 0.5λ-wide strip; UTD (dash-dotted line), MoM (dashed line), this formulation (continuous line). (a) Dipole perpendicular to the edges (hard case). (b) Dipole parallel to the edges (soft case).

VI. Concluding Remarks

A closed-form high-frequency solution has been presented for the scattering in the near zone by a pair of coplanar skew edges when they are illuminated by a source at a finite distance. For the sake of simplicity in the explanation, the formulation has been carried out for two half-planes, however, this same technique can easily be extended to treat the case of two wedges. A spectral spherical-wave representation of the first-order scattered field from the trailing edge has been employed here. An appropriate use of the spectral response of the second edge to each spherical source provides a spherical-wave/near-field, double integral representation of the doubly diffracted field. Its integrand exhibits poles that independently occur in the two variables. This property has been found very convenient to obtain the desired asymptotic form for both hard and soft boundary conditions on the two half-planes. In particular, appropriate transition functions have been introduced that involve generalized Fresnel integrals. These transition functions properly account for the slope contribution of the primary diffraction; thus, they also provide a suitable description of the double diffraction mechanism when the two edges are joined by a common face. Numerical results have shown the effectiveness of the present solution for calculating the field at any illumination and observation aspects, including overlapping transition regions. It has been found that this solution fails so gracefully that is applicable even for vanishing distance between the two diffraction points.

Appendix

To derive a high-frequency expression for the doubly diffracted field contribution ψ_{12}^{dd} (8), the variable transformation $u = \sin\frac{\alpha_1}{2}$, $v = \sin\frac{\alpha_2}{2}$, and the notation $u_p = \sin\frac{\Phi_1^p}{2}$, $v_q = \sin\frac{\Phi_2^q}{2}$ are introduced; as a consequence, retaining the even part of the integrand, namely the nonvanishing part of

the integral, leads to

$$\psi_{12}^{dd} = \sum_{p,q=1}^{2} \tilde{I}_{pq} + \tilde{\tilde{I}}_{pq} \tag{32}$$

where

$$\tilde{I}_{pq} = \int_{-j\infty}^{j\infty}\int_{-j\infty}^{j\infty} \tilde{B}_{pq}(u,v) \frac{u_p v_q e^{-jkr(u,v)}}{\left(u^2-u_p^2\right)\left(v^2-v_q^2\right)}\, du\, dv \tag{33}$$

and

$$\tilde{\tilde{I}}_{pq} = \int_{-j\infty}^{j\infty}\int_{-j\infty}^{j\infty} \tilde{\tilde{B}}_{pq}(u,v) \frac{uv e^{-jkr(u,v)}}{\left(u^2-u_p^2\right)\left(v^2-v_q^2\right)}\, du\, dv \tag{34}$$

in which

$$\tilde{B}_{pq}(u,v) = -\frac{(\pm 1)^{p+q}}{16\pi^2 r(u,v)} \tag{35}$$

and

$$\tilde{\tilde{B}}_{pq}(u,v) = -\frac{(\mp 1)^{p+q}}{16\pi^2 r(u,v)} \frac{\sqrt{1-u_p^2}\sqrt{1-v_q^2}}{\sqrt{1-u^2}\sqrt{1-v^2}} \tag{36}$$

respectively. In (35) and (36), the upper (lower) sign applies to the hard (soft) case, and $r(u,v) = R(\alpha_1, \alpha_2)$. In each term of (32), the relevant stationary phase point occurs at $(u,v) = (0,0)$; also, the integrands exhibit a symmetric pair of poles for each variable $u = \pm u_p, v = \pm v_q$.

Although both terms have the same phase and pole singularities, their integrands have a quite different behavior close to and at the stationary phase point; in particular, the integrand in $\tilde{\tilde{I}}_{pq}$ vanishes at $(u,v) = (0,0)$.

It is worth noting that both $\tilde{B}_{pq}$ and $\tilde{\tilde{B}}_{pq}$ are regular, slowly varying functions in a neighborhood of $(u,v) = (0,0)$; indeed, their gradients vanish at the stationary phase point. Introducing the Taylor quadratic expansion for the phase function $r(u,v)$ at the stationary phase point, $\tilde{I}_{pq}$ and $\tilde{\tilde{I}}_{pq}$ may asymptotically be represented as

$$\tilde{I}_{pq} \sim \frac{2\pi \tilde{B}_{pq}(0,0) e^{-jkr(0,0)}}{jk u_p v_q \left(r_{uu} r_{vv} - r_{uv}^2\right)^{1/2}} \tilde{T}(a_p, b_q, w) \tag{37}$$

and

$$\tilde{\tilde{I}}_{pq} \sim \frac{2\pi r_{uv} \tilde{\tilde{B}}_{pq}(0,0) e^{-jkr(0,0)}}{k^2 u_p^2 v_q^2 \left(r_{uu} r_{vv} - r_{uv}^2\right)^{3/2}} \tilde{\tilde{T}}(a_p, b_q, w) \tag{38}$$

respectively, where r_{uv} (r_{uu} or r_{vv}) denotes the second derivative of r with respect to u and v (u^2 or v^2) evaluated at the stationary phase point. The first factors in (37) and (38) are the nonuniform evaluation of $\tilde{I}_{pq}$ and $\tilde{\tilde{I}}_{pq}$ at the stationary phase point, respectively, while

$$\tilde{T}(a,b,w) = \frac{a^2 b^2}{j\pi (1-w^2)^{3/2}} \times \int_{-\infty}^{\infty}\int_{-\infty}^{\infty} \frac{e^{j(\xi^2 + 2w\xi\eta + \eta^2)}}{\left(\xi^2 - \frac{a^2}{1-w^2}\right)\left(\eta^2 - \frac{b^2}{1-w^2}\right)}\, d\xi\, d\eta \tag{39}$$

and

$$\tilde{\tilde{T}}(a,b,w) = \frac{2a^2 b^2}{\pi w (1-w^2)^{1/2}} \times \int_{-\infty}^{\infty}\int_{-\infty}^{\infty} \frac{\xi\eta e^{j(\xi^2 + 2w\xi\eta + \eta^2)}}{\left(\xi^2 - \frac{a^2}{1-w^2}\right)\left(\eta^2 - \frac{b^2}{1-w^2}\right)}\, d\xi\, d\eta \tag{40}$$

are the relevant transition functions, respectively; their arguments are

$$a_p = j u_p \sqrt{\frac{1}{2} r_{uu}(1-w^2)} \quad b_q = j v_q \sqrt{\frac{1}{2} r_{vv}(1-w^2)} \tag{41}$$

where

$$w = \frac{|r_{uv}|}{\sqrt{r_{uu} r_{vv}}}. \tag{42}$$

By means of proper manipulations, similar to those in [18], (39) and (40) can be expressed in terms of GFI's (19) leading to (17) and (18), respectively, while (41) and (42) yield (20) and (21). To calculate $\tilde{\tilde{T}}(a,b,w)$, the algorithm suggested in [14] has to be slightly modified by using the more accurate approximation

$$G_3(x,y) = \frac{1}{2\pi} \frac{y}{2jx(x^2+y^2)} \left[1 - \frac{3x^2+y^2}{x(x^2+y^2)} \frac{F(x^2)}{2jx}\right] \tag{43}$$

in place of [14, Eq. (11)], where $F(x)$ is the UTD transition function [1].

The following relationships are useful for investigating the behavior of our solution in the various transition regions addressed in Section V-A. When the observation point approaches the aspect angle $\phi_2 = \phi'_{12} + \pi$, $b_1 \to 0$, consequently [14]

$$\tilde{T}(a_p, b_1 \to 0, w) \simeq \sqrt{j\pi}\, |b_1| F\left(\frac{a_p^2}{1-w^2}\right) \tag{44}$$

which leads to (24) and

$$\tilde{\tilde{T}}(a_p, b_1 \to 0, w) \simeq \frac{-8 a_p^2 b_1^2}{w\sqrt{1-w^2}} \mathcal{G}\left(a_p, \frac{w a_p}{\sqrt{1-w^2}}\right). \tag{45}$$

When (45) is introduced into (16), the following expression for $\tilde{\tilde{\psi}}_{12}^{dd}$ is obtained for $\Phi_2^1 = 2\pi$

$$\tilde{\tilde{\psi}}_{12}^{dd} = \psi\{P', O_1\} \frac{-\epsilon_{12} r'_1 e^{-jk(\ell + r_2)}}{(r'_1 + \ell + r_2)} \sum_{p=1}^{2} (\pm 1)^{p+1} \cos\left(\frac{\Phi_1^p}{2}\right) \times \mathcal{G}\left(a_p, \frac{w a_p}{\sqrt{1-w^2}}\right) + O(k^{-2}) \tag{46}$$

which shows that the two terms with $q = 1$ provide a continuous contribution of order k^{-1} with respect to the incident field. Higher order contributions (k^{-2}) are given by the two remaining terms with $q = 2$.

Let us next consider the plane containing the two edges where $\phi'_1 = \pi + \phi_{12}$ and $\phi_2 = \phi'_{12} + \pi$ and assume that both the source and the observation points approach those aspects from the lit region of the incident and the singly diffracted fields. It is rather apparent that the leading terms of the UTD description of the two singly diffracted fields tend to cancel the incident field. At these same aspects, using the small argument

expansion of the $\tilde{T}$ transition function

$$\tilde{T}(a_1 \to 0, b_1 \to 0, w) \simeq \frac{j\pi|a_1||b_1|}{\sqrt{1-w^2}} \tag{47}$$

leads to expression (25), which provides $1/4$ of the incident field. In this case, the term $pq = 21$ in (15), as well as its corresponding term $pq = 12$, are of order $k^{-1/2}$ and provide the continuity for the GO shadowing of the nonleading terms of the UTD singly diffracted fields from edges 1 and 2, respectively.

Finally, let us consider the field contribution $\tilde{\tilde{\psi}}_{12}^{dd}$. Equation (26), for its leading term $pq = 11$, is obtained by using the small arguments approximation for the transition function

$$\tilde{\tilde{T}}(a_1 \to 0, b_1 \to 0, w) \simeq \frac{-4a_1^2 b_1^2}{w\sqrt{1-w^2}} \sin^{-1} w. \tag{48}$$

ACKNOWLEDGMENT

The authors would like to thank Prof. R. J. Marhefka for stimulating discussions and Dr. R. Cioni from Ingegneria dei Sistemi (IDS), Pisa, Italy, for providing the MoM results.

REFERENCES

[1] R. G. Kouyoumjian and P. H. Pathak, "A uniform geometrical theory of diffraction for an edge in a perfectly conducting surface," *Proc. IEEE*, vol. 62, pp. 1448–1461, Nov. 1974.
[2] G. L. James and G. D. Poulton, "Double knife-edge diffraction for curved, screens," *Microwaves, Opt., Acoust.*, vol. 3, pp. 221–223, 1979.
[3] R. Tiberio and R. G. Kouyoumjian, "A uniform GTD solution for the diffraction by strips illuminated at grazing incidence," *Radio Sci.*, vol. 14, pp. 933–941, 1979.
[4] ——, "An analysis of diffraction at edges illuminated by transition region fields," *Radio Sci.*, vol. 17, pp. 323–336, 1982.
[5] R. Tiberio, G. Manara, G. Pelosi, and R. Kouyoumjian, "High-frequency electromagnetic scattering of plane waves from double wedges," *IEEE Trans. Antennas Propagat.*, vol. 37, pp. 1172–1180, Sept. 1989.
[6] M. Schneider and R. Luebbers, "A general UTD diffraction coefficient for two wedges," *IEEE Trans. Antennas Propagat.*, vol. 39, pp. 8–14, Jan. 1991.
[7] A. Michaeli, "A new, asymptotic high-frequency analysis of electromagnetic scattering by a pair of parallel edges-closed form results," *Radio Sci.*, vol. 20, pp. 1537–1548, 1985.
[8] ——, "A hybrid asymptotic solution for the scattering by a pair of perfectly conducting wedges," *IEEE Trans. Antennas Propagat.*, vol. 38, pp. 664–667, May 1990.
[9] L. P. Ivrissimtzis and R. J. Marhefka, "Double diffraction at a coplanar skewed edge configuration," *Radio Sci.*, vol. 26, pp. 821–830, 1991.
[10] L. P. Ivrissimtzis and R. J. Marhefka, "A uniform ray approximation of the scattering by polyhedral structures including higher terms," *IEEE Trans. Antennas Propagat.*, vol. 40, pp. 1302–1312, Nov. 1992.
[11] P. H. Pathak and R. G. Kouyoumjian, "The dyadic diffraction coefficient for a perfectly conducting wedge," Tech. Rep. 5, The Ohio State Univ., ElectroSci. Lab., Dept. Elect. Eng., June 1970 (under U.S. Airforce Contract AF19(628)-5929).
[12] L. Felsen and N. Marcuvitz, *Radiation and Scattering of Waves*. Englewood Cliffs, NJ: Prentice-Hall, 1973..
[13] S. Maci, R. Tiberio, and A. Toccafondi, "Diffraction at a plane angular sector," *J. Electromagn. Wave Applicat.*, vol. 8, no. 9/10, pp. 1247–1276, Sept./Oct. 1994.
[14] F. Capolino and S. Maci, "Simplified, closed-form expressions for computing the generalized Fresnel integral and their application to vertex diffraction," *Microwave Opt. Tech. Lett.*, vol. 9, no. 1, pp. 32–37, 1995.
[15] ——, "Uniform high-frequency description of singly, doubly, and vertex diffracted rays for a plane angular sector," *J. Electromagn. Wave Applicat.*, vol. 10, no. 9, pp. 1175–1197, Oct. 1996.
[16] M. Albani, F. Capolino, S. Maci, and R. Tiberio, "Diffraction at a thick screen including corrugations on the top face," *IEEE Trans. Antennas Propagat.*, vol. 45, pp. 277–283, Feb. 1997.
[17] S. W. Lee and J. Boersma, "Ray-optical analysis of fields on shadow boundaries of two parallel plates," *J. Math. Phys.*, vol. 16, pp. 1746–1764, 1975.
[18] K. H. Hill, "A UTD solution to the EM scattering by the vertex of a perfectly conducting plane angular sector," Ph.D. dissertation, The Ohio State Univ., Dept. Elect. Eng., 1990.

Filippo Capolino (S'94–M'97) was born in Florence, Italy, in 1967. He received the doctor degree (*cum laude*) in electronic engineering from the University of Florence, Italy, and the Ph.D. degree from the same university, in 1993 and 1997, respectively.

From 1994 to 1996, he was an Instructor at the University of Siena, Italy He is now an Adjunct Professor at the same university. His research interests mainly concern theoretical and applied electromagnetics, in particular with high-frequency methods for electromagnetic scattering, and electromagnetic models of random surfaces.

Dr. Capolino won the MMET'94 Student Paper Award in 1994 and in 1996 he won the Raj Mittra Travel Grant for Young Scientists and the "Barzilai" prize for the best paper at the National Italian Congress of Electromagnetism (XI RiNEm).

Matteo Albani was born in Florence, Italy, in 1970. He received the doctor degree (*cum laude*) in electronic engineering from the University of Florence, Italy, in 1994.

He is presently involved with a Ph.D. research program at the University of Siena, concerning the high-frequency methods for the electromagnetic scattering and diffraction. His research interests are also focused on numerical methods for electromagnetics.

Dr. Albani received a special award for his thesis work from the University of Florence.

Stefano Maci (M'92) was born in Rome, Itlay, in 1961. He received the doctor degree in electronic engineering from the University of Florence, Italy, in 1987.

In 1990, he joined the Department of Electronic Engineering of the University of Florence as Assistant Professor. Since 1993 he has also been an Adjunct Professor at the University of Siena, Italy. In 1997 he was an Invited Professor at the Technical University of Denmark, Copenhagen. His interests are focused on electromagnetic theory, mainly concerning high- and low-frequency methods for antennas and electromagnetic scattering. He has also developed research activity on specific topics concerning microwaves antennas, particularly focused on the analysis, synthesis, and design of patch antennas.

Dr. Maci received the National Young Scientists "Francini" Award for the Laurea thesis in 1988 and in the 1996 he was awarded with the "Barzilai" prize for the best paper at the National Italian Congress of Electromagnetism (XI RiNEm).

Roberto Tiberio (M'81–SM'83–F'93) was born in Rome, Italy, in 1946. He received the doctor degree (*cum laude*) from the University of Pisa, Italy, in 1970.

In 1972, he joined the Department of Electronic Engineering of the University of Florence, Italy, where he was a Full Professor until October 1993. Next, he joined the University of Siena, Italy, where he is the Dean of the College of Engineering. Since 1976 he has been collaborating with the Electroscience Laboratory of The Ohio State University, Columbus, where he worked continuously as a Senior Research Assistant for two years and then periodically as a Scientific Consultant. His research interests are focused on electromagnetic theory and high-frequency methods, mainly concerning the development and applications of analytic and numerical techniques for antenna design and RCS prediction.

Dr. Tiberio is an Italian Delegate of URSI (Commission B).